

Quasi-Gasdynamics Equations and Numerical Simulation of Viscous Gas Flows

T. G. Elizarova*, M. E. Sokolova**, and Yu. V. Sheretov***

* Institute for Mathematical Modeling, Russian Academy of Sciences,
 Miusskaya pl. 4a, Moscow, 125047 Russia
 e-mail: elizar@imamod.ru

** Faculty of Physics, Moscow State University, Leninskie gory, Moscow, 119992 Russia
 e-mail: msokolova@imamod.ru

*** Tver State University, ul. Zhelyabova 33, Tver, 170000 Russia
 e-mail: Yurii.Sheretov@tversu.ru

Received June 30, 2004; in final form, September 30, 2004

Abstract—The system of quasi-gasdynamics equations and an entropy balance equation are presented. Numerical methods are described for solving the equations, which are used to simulate subsonic and supersonic viscous unsteady gas flows. Two-dimensional flows are computed as examples.

Keywords: numerical simulation, viscous gas, subsonic and supersonic flows.

INTRODUCTION

The system of quasi-gasdynamics (QGD) equations expands the capabilities of the classical Navier–Stokes model for describing viscous compressible gas flows. This system was first derived in [1] on the basis of a well-known kinetic model. A flow was represented as collisionless motion of gas atoms followed by instantaneous relaxation to a local equilibrium state. In [2–4], the differential QGD equations were phenomenologically derived from integral conservation laws written for a moving material volume and the properties of the QGD system were examined. It was found that the QGD equations are well suited for simulation of flows in which the gasdynamic parameters do not vary widely with time. Since the first publications on this subject, numerical methods for solving the QGD equations have been developed and kinetically consistent finite-difference schemes, which are closely related to the QGD equations, have been analyzed [5].

In this study, the QGD equations are written out in an inversion form that corresponds to differential conservation laws and an entropy balance equation is given. The modern view of numerical methods for these equations as applied to unsteady supersonic and subsonic flows is presented, and some examples of computation of two-dimensional problems are given.

1. QUASI-GASDYNAMIC SYSTEM OF EQUATIONS

Taking into account the external forces, the QGD system can be represented in inversion form:

$$\frac{\partial \rho}{\partial t} + \operatorname{div} \mathbf{j}_m = 0, \quad (1.1)$$

$$\frac{\partial(\rho u)}{\partial t} + \operatorname{div}(\mathbf{j}_m \otimes u) + \nabla p = \rho_* \mathbf{F} + \operatorname{div} \Pi, \quad (1.2)$$

$$\frac{\partial}{\partial t} \left[\rho \left(\frac{\mathbf{u}^2}{2} + \varepsilon \right) \right] + \operatorname{div} \left[\mathbf{j}_m \left(\frac{\mathbf{u}^2}{2} + \varepsilon + \frac{p}{\rho} \right) \right] + \operatorname{div} \mathbf{q} = (\mathbf{j}_m \cdot \mathbf{F}) + \operatorname{div}(\Pi \cdot \mathbf{u}). \quad (1.3)$$

The system is closed by the equations of state of an ideal polytropic gas:

$$p = \rho RT, \quad \varepsilon = c_v T, \quad s = c_v \ln \left(\frac{RT}{\rho^{(\gamma-1)}} \right) + \text{const}. \quad (1.4)$$

Here, $\rho = \rho(\mathbf{x}, t)$ is the density of the medium, $\mathbf{u} = \mathbf{u}(\mathbf{x}, t)$ is the velocity, $p = p(\mathbf{x}, t)$ is the pressure, $\varepsilon = \varepsilon(\mathbf{x}, t)$ is the specific internal energy, $T = T(\mathbf{x}, t)$ is the temperature, $s = s(\mathbf{x}, t)$ is the specific entropy, $\mathbf{F} = \mathbf{F}(\mathbf{x})$

is the body density of external forces, $\rho_* = \rho - \tau \operatorname{div}(\rho \mathbf{u})$ is an approximate value of the density at the point $(\mathbf{x}, t + \tau)$, R is the universal gas constant, $c_v = R/(\gamma - 1)$ is the heat capacity at a constant pressure, and γ is the adiabatic index. The symbols \otimes and \cdot stand for the direct tensor product and the scalar product, respectively. The quantities $\mathbf{j}_m = \mathbf{j}_m(\mathbf{x}, t)$, $\Pi = \Pi(\mathbf{x}, t)$, and $q = q(\mathbf{x}, t)$ are interpreted as the mass flux density, the viscous stress tensor, and the heat flux, respectively, and they are calculated by the formulas

$$\mathbf{j}_m = \rho(\mathbf{u} - \mathbf{w}), \tag{1.5}$$

$$\Pi = \Pi_{\text{NS}} + \tau \mathbf{u} \otimes [\rho(\mathbf{u} \cdot \nabla) \mathbf{u} + \nabla \rho - \rho \mathbf{F}] + \tau I[(\mathbf{u} \cdot \nabla) p + \gamma p \operatorname{div} \mathbf{u}], \tag{1.6}$$

$$q = q_{\text{NS}} - \tau \rho \mathbf{u} [(\mathbf{u} \cdot \nabla) \varepsilon + p(\mathbf{u} \cdot \nabla)(1/\rho)], \tag{1.7}$$

where

$$\Pi_{\text{NS}} = \mu [(\nabla \otimes \mathbf{u}) + (\nabla \otimes \mathbf{u})^T - (2/3)I \operatorname{div} \mathbf{u}], \tag{1.8}$$

$$\mathbf{q}_{\text{NS}} = -\kappa \nabla T, \tag{1.9}$$

$$\mathbf{w} = \frac{\tau}{\rho} [\operatorname{div}(\rho \mathbf{u} \otimes \mathbf{u}) + \nabla p - \rho \mathbf{F}]. \tag{1.10}$$

The functions $\mu = \mu(T)$, $\kappa = \kappa(T)$, and $\tau = \tau(p, T)$ are defined as

$$\mu = \mu_1 \left(\frac{T}{T_1} \right)^\omega, \quad \kappa = \frac{c_p \mu}{\text{Pr}}, \quad \tau = \frac{\mu}{p \text{Sc}}, \tag{1.11}$$

where μ_1 is a given dynamic viscosity at temperature T_1 , ω is a given power-law parameter, $c_p = \gamma R/(\gamma - 1)$ is the specific heat capacity at constant pressure, Pr is the Prandtl number, and Sc is the Schmidt number.

When $\tau = 0$, the QGD equations become the Navier–Stokes equations.

It was shown in [2, 3] that QGD system (1.1)–(1.11) is dissipative and an entropy balance equation can be derived for it. To obtain this equation, Eqs. (1.1)–(1.3) were represented in [3] in nonconservative form:

$$\rho D(1/\rho) = \operatorname{div}(\mathbf{u} - \mathbf{w}), \tag{1.12}$$

$$\rho D\mathbf{u} + \nabla p = \rho_* \mathbf{F} + \operatorname{div} \Pi, \tag{1.13}$$

$$\rho D(\mathbf{u}^2/2 + \varepsilon) + (\mathbf{u} - \mathbf{w}) \cdot \nabla p + p \operatorname{div}(\mathbf{u} - \mathbf{w}) + \operatorname{div} \mathbf{q} = \rho(\mathbf{u} - \mathbf{w}) \cdot \mathbf{F} + \operatorname{div}(\Pi \cdot \mathbf{u}). \tag{1.14}$$

Here, $D = \partial/\partial t + (\mathbf{u} - \mathbf{w}) \cdot \nabla$ is a differential operator. By using the tensor analysis rules, the entropy balance equation is derived from Eqs. (1.12)–(1.14) to be

$$\rho Ds = -\operatorname{div}(\mathbf{q}/T) + X, \tag{1.15}$$

where the nonnegative entropy production is defined by the formula

$$\begin{aligned} X = & \kappa \left(\frac{\nabla T}{T} \right)^2 + \frac{(\Pi_{\text{NS}} : \Pi_{\text{NS}})}{2\mu T} + \frac{p\tau}{\rho^2 T} [\operatorname{div}(\rho \mathbf{u})]^2 \\ & + \frac{\tau}{\rho T} [\rho(\mathbf{u} \cdot \nabla) \mathbf{u} + \nabla p - \rho \mathbf{F}]^2 + \frac{\tau}{\rho \varepsilon T} [\rho(\mathbf{u} \cdot \nabla) \varepsilon + p \operatorname{div} \mathbf{u}]^2, \end{aligned} \tag{1.16}$$

in which $(\Pi_{\text{NS}} : \Pi_{\text{NS}}) = \sum_{i,j=1}^3 (\Pi_{\text{NS}})_{ij} (\Pi_{\text{NS}})_{ij}$ is the double scalar product of two identical tensors. Note that the terms involving τ in (1.16) are the squared left-hand sides of the classical time-independent Euler equations with positive coefficients. By using the mass conservation law (1.1), identity (1.15) can be represented in conservative form:

$$\frac{\partial(\rho s)}{\partial t} + \operatorname{div}(\mathbf{j}_m s) = -\operatorname{div} \left(\frac{\mathbf{q}}{T} \right) + X. \tag{1.17}$$

Consider a gas flow within a closed vessel V_0 with a thermally nonconductive wall Σ_0 . System (1.1)–(1.11) is supplemented with the initial conditions

$$\rho|_{t=0} = \rho_0, \quad \mathbf{u}|_{t=0} = u_0, \quad T|_{t=0} = T_0, \quad \mathbf{x} \in V_0, \tag{1.18}$$

and the boundary conditions

$$\mathbf{u}|_{\Sigma_0} = 0, \quad (\mathbf{j}_m \cdot \mathbf{n})|_{\Sigma_0} = 0, \quad (\mathbf{q} \cdot \mathbf{n})|_{\Sigma_0} = 0, \quad t \geq 0. \quad (1.19)$$

Here, $\rho_0 = \rho_0(\mathbf{x}) > 0$, $\mathbf{u}_0 = \mathbf{u}_0(\mathbf{x})$, and $T_0 = T_0(\mathbf{x}) > 0$ are the given density, velocity, and temperature at the time $t = 0$. The first condition in (1.19) means that the gas adheres to the vessel's walls, the second condition ensures no mass flux through the boundary, and the third condition implies that the normal component of the heat flux is zero on Σ_0 . Integrating (1.17) and taking into account (1.18) and (1.19), we obtain an inequality for the total thermodynamic entropy $S(t) = \int_{V_0} (\rho s) d\mathbf{x}$:

$$dS(t)/dt \geq 0. \quad (1.20)$$

It follows from (1.20) that $S(t)$ is a nondecreasing function of time. A similar fact is known to hold for the Navier–Stokes system.

An asymptotic analysis performed in [2, 3] for the QGD system with the Knudsen number tending to zero showed that, for steady flows, the additional terms proportional to τ are $o(\text{Kn}^2)$ quantities; i.e., in the limit of a vanishing Knudsen number, QGD equations (1.1)–(1.11) become the Navier–Stokes equations. Recall that the Knudsen number is defined as $\text{Kn} = \lambda/L$ (where λ is the mean free path in an unperturbed flow and L is the characteristic length).

For Kn tending to unity and for rapidly varying flows, the additional dissipative terms can have a larger effect. In the boundary-layer approximation, the QGD equations, as well as the Navier–Stokes equations, are transformed into the Prandtl equations.

Because of the no-slip and impermeability conditions imposed (see the first two relations in (1.19)), the additional dissipation in the QGD equations is nonzero only in the flow domain and vanishes on the boundary of the domain. In particular, for the QGD equations, the heat flux toward the wall and the off-diagonal components of the viscous stress tensor, which determine friction on the boundary, coincide with the corresponding quantities for the Navier–Stokes equations.

2. FINITE-DIFFERENCE APPROXIMATION OF THE QGD EQUATIONS

A finite-difference approximation to the QGD equations is constructed using the QGD system written as conservation laws (1.1)–(1.3). Unlike previously developed methods, the approximations are constructed in the flux form for the mass flux density \mathbf{j}_m , the heat flux \mathbf{q} , and the viscous stress tensor Π written in the form of (1.5)–(1.10), which makes the numerical algorithm compact and economic. As a result, the values of the viscosity, heat conductivity, and relaxation parameter in the additional QGD terms can be varied independently [6, 7].

For two-dimensional flows, the QGD equations are given by

$$\begin{aligned} \frac{\partial \rho}{\partial t} + \frac{\partial j_{mx}}{\partial x} + \frac{\partial j_{my}}{\partial y} &= 0, \\ \frac{\partial(\rho u_x)}{\partial t} + \frac{\partial(j_{mx}u_x)}{\partial x} + \frac{\partial(j_{my}u_x)}{\partial y} + \frac{\partial p}{\partial x} &= \frac{\partial \Pi_{xx}}{\partial x} + \frac{\partial \Pi_{yx}}{\partial y}, \\ \frac{\partial(\rho u_y)}{\partial t} + \frac{\partial(j_{mx}u_y)}{\partial x} + \frac{\partial(j_{my}u_y)}{\partial y} + \frac{\partial p}{\partial y} &= \frac{\partial \Pi_{xy}}{\partial x} + \frac{\partial \Pi_{yy}}{\partial y}, \\ \frac{\partial E}{\partial t} + \frac{\partial(j_{mx}H)}{\partial x} + \frac{\partial(j_{my}H)}{\partial y} + \frac{\partial q_x}{\partial x} + \frac{\partial q_y}{\partial y} &= \frac{\partial}{\partial x}(\Pi_{xx}u_x + \Pi_{xy}u_y) + \frac{\partial}{\partial y}(\Pi_{yx}u_x + \Pi_{yy}u_y). \end{aligned} \quad (2.1)$$

Here, u_x and u_y are the projections of the velocity u onto the x and y axis, respectively; E is the total energy of a unit volume; and H is the total specific enthalpy. The last two quantities are calculated by the formulas

$$E = \rho \frac{u_x^2 + u_y^2}{2} + \frac{p}{\gamma - 1}, \quad H = \frac{E + p}{\rho}.$$

The components of the mass flux density, j_{mx} and j_{my} , are calculated as

$$j_{mx} = \rho(u_x - w_x), \quad j_{my} = \rho(u_y - w_y), \quad (2.2)$$

where

$$w_x = \frac{\tau}{\rho} \left[\frac{\partial(\rho u_x^2)}{\partial x} + \frac{\partial(\rho u_x u_y)}{\partial y} + \frac{\partial p}{\partial x} \right], \quad w_y = \frac{\tau}{\rho} \left[\frac{\partial(\rho u_x u_y)}{\partial x} + \frac{\partial(\rho u_y^2)}{\partial y} + \frac{\partial p}{\partial y} \right].$$

The components of Π are determined by the formulas

$$\begin{aligned} \Pi_{xx} &= \Pi_{xx}^{\text{NS}} + u_x w_x^* + R^*, & \Pi_{xx}^{\text{NS}} &= 2\mu \frac{\partial u_x}{\partial x} - \frac{2}{3}\mu \operatorname{div} \mathbf{u}, \\ \Pi_{xy} &= \Pi_{xy}^{\text{NS}} + u_x w_y^*, & \Pi_{xy}^{\text{NS}} = \Pi_{yx}^{\text{NS}} &= \mu \left(\frac{\partial u_y}{\partial x} + \frac{\partial u_x}{\partial y} \right), \\ \Pi_{yx} &= \Pi_{yx}^{\text{NS}} + u_y w_x^*, \\ \Pi_{yy} &= \Pi_{yy}^{\text{NS}} + u_y w_y^* + R^*, & \Pi_{yy}^{\text{NS}} &= 2\mu \frac{\partial u_y}{\partial y} - \frac{2}{3}\mu \operatorname{div} \mathbf{u}, \end{aligned} \quad (2.3)$$

and w_x^* , w_y^* , R^* , and the divergence of the velocity ($\operatorname{div} \mathbf{u}$) are given by the formulas

$$\begin{aligned} w_x^* &= \tau \left(\rho u_x \frac{\partial u_x}{\partial x} + \rho u_y \frac{\partial u_y}{\partial y} + \frac{\partial p}{\partial x} \right), & w_y^* &= \tau \left(\rho u_x \frac{\partial u_y}{\partial x} + \rho u_y \frac{\partial u_y}{\partial y} + \frac{\partial p}{\partial y} \right), \\ R^* &= \tau \left(u_x \frac{\partial p}{\partial x} + u_y \frac{\partial p}{\partial y} + \gamma p \operatorname{div} \mathbf{u} \right), & \operatorname{div} \mathbf{u} &= \frac{\partial u_x}{\partial x} + \frac{\partial u_y}{\partial y}. \end{aligned} \quad (2.4)$$

The components of the heat flux q are calculated as

$$\begin{aligned} q_x &= q_x^{\text{NS}} - u_x R^q, & q_y &= q_y^{\text{NS}} - u_y R^q, \\ R^q &= \tau \rho \left[\frac{u_x}{\gamma - 1} \frac{\partial}{\partial x} \left(\frac{p}{\rho} \right) + \frac{u_y}{\gamma - 1} \frac{\partial}{\partial y} \left(\frac{p}{\rho} \right) + p u_x \frac{\partial}{\partial x} \left(\frac{1}{\rho} \right) + p u_y \frac{\partial}{\partial y} \left(\frac{1}{\rho} \right) \right], \end{aligned} \quad (2.5)$$

where the Navier–Stokes terms q_x^{NS} and q_y^{NS} are given by the formulas

$$q_x^{\text{NS}} = -\kappa \frac{\partial T}{\partial x}, \quad q_y^{\text{NS}} = -\kappa \frac{\partial T}{\partial y}.$$

System (2.1)–(2.5) is supplemented with initial and boundary conditions.

To solve the problem numerically, a grid in space and time is introduced in the computational domain. The components of the velocity, pressure, and density are determined at the nodes of the grid. The values of the gasdynamic characteristics $\Psi = (\rho, u_x, u_y, p)$ at the nodes with half-integer indices and at the cells' centers are determined as the arithmetic mean of their values at the adjacent nodes:

$$\begin{aligned} \Psi_{i \pm 1/2, j} &= 0.5(\Psi_{i \pm 1, j} + \Psi_{i, j}), & \Psi_{i, j \pm 1/2} &= 0.5(\Psi_{i, j \pm 1} + \Psi_{i, j}), \\ \Psi_{i+1/2, j \pm 1/2} &= 0.25(\Psi_{i+1, j \pm 1} + \Psi_{i, j \pm 1} + \Psi_{i+1, j} + \Psi_{i, j}), \\ \Psi_{i-1/2, j \pm 1/2} &= 0.25(\Psi_{i-1, j \pm 1} + \Psi_{i, j \pm 1} + \Psi_{i-1, j} + \Psi_{i, j}). \end{aligned}$$

For the remaining functions $f = f(\rho, u_x, u_y, p)$, we set $f = f(\rho_{ij}, (u_x)_{ij}, (u_y)_{ij}, p_{ij})$. Similar relations also hold for nodes with half-integer indices.

Initial–boundary value problem (2.1) is solved by applying a finite-difference scheme that is explicit in time. The spatial derivatives are approximated by central differences with second-order accuracy, and the time derivatives are approximated by forward differences with first-order accuracy.

The first equation in system (2.1) is approximated by

$$\frac{\hat{\rho}_{ij} - \rho_{ij}}{\Delta t} + \frac{1}{h_x} [(j_{mx})_{i+1/2, j} - (j_{mx})_{i-1/2, j}] + \frac{1}{h_y} [(j_{my})_{i, j+1/2} - (j_{my})_{i, j-1/2}] = 0,$$

where Δt is the time step and $\hat{\rho}_{ij}$ is calculated at the succeeding time level. The other equations in system (2.1) are approximated in a similar manner.

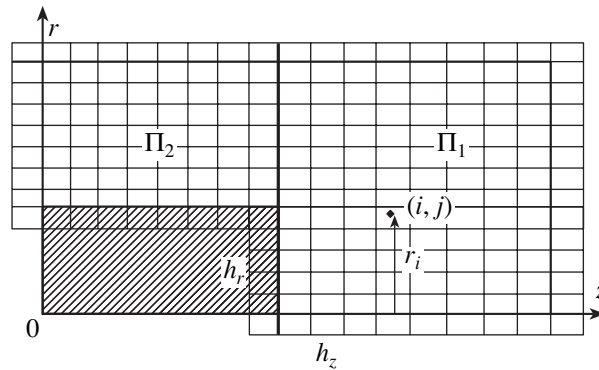


Fig. 1.

To obtain a unified procedure for computing gasdynamic characteristics at all the interior points, including the near-boundary ones, we introduce a set of fictitious cells adjacent to each boundary. If the computational domain consists of rectangular subdomains, then, for an accurate approximation of the equations near the corner points, the computational domain is divided into the corresponding rectangular subdomains and fictitious cells are introduced along their boundaries [6]. An algorithm for finding the density, velocity components, and pressure consists of two steps. At the first, the values in the fictitious cells are determined from the boundary conditions. At the second step, the flow variables at the interior points are computed at the next time level. To solve the initial–boundary value problem numerically, we use a finite-difference scheme with explicit time differencing. Figure 1 shows an example of partitioning the computational domain and the location of the fictitious cells for an axisymmetric flow.

3. NUMERICAL SIMULATION OF SUPERSONIC FLOWS

To compute supersonic flows, QGD equations (2.1)–(2.5) are nondimensionalized using the following reference parameters: the free-stream density ρ_∞ , the free-stream velocity c_∞ , and the reference length L . The relations between the dimensional and nondimensional characteristics (the latter are marked with a tilde) are given by

$$\rho = \tilde{\rho}\rho_\infty, \quad u = \tilde{u}c_\infty, \quad p = \tilde{p}\rho_\infty c_\infty^2, \quad x = \tilde{x}L, \quad t = \tilde{t}\frac{L}{c_\infty}, \quad T = \tilde{T}\frac{c_\infty^2}{\gamma R}. \quad (3.1)$$

The Mach and Reynolds numbers are defined as

$$M = \frac{u_\infty}{c_\infty}, \quad \text{Re} = \frac{u_\infty \rho_\infty L}{\mu_0},$$

where $c_\infty = \sqrt{\gamma R T_\infty}$ is the speed of sound at the temperature T_∞ .

After nondimensionalization, system (2.1)–(2.5) does not change in form. The coupling equations become $p = \rho T / \gamma$ and $c = \sqrt{T}$.

To ensure the stability of a numerical solution, a term proportional to the mesh size is added to τ . Then, the relaxation parameter, viscosity, and heat conductivity are calculated as

$$\tau = \frac{M}{\text{ReSc}p} \frac{1}{(\rho\gamma)^\omega} + \alpha \frac{h_{xy}}{c}, \quad \mu = p\text{Sc}\tau, \quad \kappa = \frac{\tau p \text{Sc}}{\text{Pr}(\gamma - 1)}, \quad (3.2)$$

where $h_{xy} = \sqrt{h_x^2 + h_y^2}$ with h_x and h_y being the mesh sizes in the x and y directions and α is a numerical factor on the order of unity.

In this numerical algorithm, the viscosity and heat conductivity are calculated by using τ . Thus, in the computational algorithm for supersonic flows, the stabilizing grid term $\alpha h_{xy}/c$ is involved in viscosity and heat conductivity.

Based on formulas (3.2), a condition can be written under which the additional grid term does not exceed the natural viscosity. Neglecting the constants on the order of unity, we obtain a condition under which the additional term can be assumed to be small:

$$\alpha \frac{h_{xy}}{c} < \frac{M}{\text{Re} \rho} \left(\frac{p}{\rho} \right)^\omega.$$

When $\omega = 1/2$, this condition simplifies to $\alpha h_{xy} < M/(\rho \text{Re})$.

The algorithm described was tested by computing the uniform supersonic flow of a viscous compressible gas over a cylinder end placed at a zero angle of attack [7]. The computational domain for this problem is schematically shown in Fig. 1. The characteristic linear size in this problem was the radius of the cylinder. The problem was solved using an analogue of system (2.1)–(2.5) written in cylindrical coordinates [6, 7]. The boundary conditions at the inlet (right) boundary corresponded to the free stream: $\rho_\infty = 1$, $(u_z)_\infty = -M$, $(u_r)_\infty = 0$, and $p_\infty = 1/\gamma$. The symmetry conditions were set on the axis of symmetry, and conditions (1.19) were set at the end face and the lateral surface of the cylinder. Mild boundary conditions (i.e., the zero normal derivatives of the density, pressure, and velocity components) were specified at the free upper and outlet (left) boundaries. The initial conditions were set using the free-stream characteristics. We considered a flow of a viscous monatomic gas consisting of rigid spheres with parameters $\gamma = 5/3$, $\text{Pr} = 2/3$, $\text{Sc} = 0.77$, $\omega = 0.5$, and $\text{Re} = 10^4$.

The computations were performed on uniform spatial grids with the mesh sizes $h_r = h_z = 0.05$ and 0.025 for $0.2 < \alpha < 1$ and $M = 1.5, 2, 3, 5, 50$. The steady-state solution was found by the relaxation method. In all the computations, the time step Δt ranged between 10^{-3} and 10^{-6} . The time step decreased with increasing Mach number and reducing mesh size. The accuracy of the solution was estimated from the computed deceleration and the position of the shock wave in front of the cylinder end. In the analyzed range of α , the accuracy of the solution and the convergence rate of the numerical algorithm little depended on α . The optimal value was $\alpha = 0.5$. The method demonstrated high accuracy in the computation of shock waves and no oscillations of the solution at high Mach numbers [7].

Equations (2.1)–(2.5) were used to compute a supersonic flow in a channel with a step. The complex geometry of the shock waves developing in the channel serves as a well-known test for evaluating solution methods designed for the Euler and Navier–Stokes equations [8, 9].

The problem was solved in the following setting: the length of the channel was equal to 3, its width was 1, and the height of the step (located a distance 0.6 from the channel) was equal to 0.2. The gas was assumed to be inviscid and thermally nonconductive with the adiabatic index $\gamma = 1.4$. A uniform flow with $M = 3$ was set on the inlet (right) boundary, and the mild boundary conditions were specified on the outlet (left) boundary. The reflecting boundary conditions were set on the walls of the channel and the step. In the computation of τ , we set $\alpha = 0.3$. Figure 2 shows the relaxation of the flow (density distribution) to a steady state as computed on a 240×80 grid. The flow pattern at the time $t = 4$ corresponds to the data obtained using high-order accurate finite-difference schemes [8, 9]. Figure 3 displays the density distributions in the channel at $t = 4$, which demonstrate the convergence of the numerical solution as the spatial grid condenses. The mesh sizes were specified as $h_x = h_y = 0.025, 0.0125$, and 0.00625 . The time steps Δt in dimensionless units were set equal to $10^{-3}, 5 \times 10^{-4}$, and 10^{-4} , respectively.

4. FEATURES OF THE ALGORITHM FOR COMPUTING SUBSONIC FLOWS

In the computation of subsonic flows, in contrast to (3.1), the reference velocity is defined as the free-stream velocity u_∞ . The dimensionless viscosity, heat conductivity, and τ are calculated by the formulas

$$\mu = \frac{1}{\text{Re}} (M^2 T)^\omega, \quad \tau = \frac{\mu}{p \text{Sc}}, \quad \kappa = \frac{\mu}{\text{Pr}(\gamma - 1)}.$$

In contrast to the algorithm for computing supersonic flows, in the case of subsonic flows, the additional stabilizing term $\alpha h_{xy}/c$ (proportional to the mesh size) is introduced only in the relaxation parameter:

$$\tau = \frac{1}{\text{Re}} \frac{1}{p \text{Sc}} (M^2 T)^\omega + \alpha h_{xy} M.$$

This term can be assumed to be small compared with the actual viscosity if $\alpha h_{xy} < M/\text{Re}$. This term is not involved in the formulas for calculating the friction and the heat flux toward the wall.

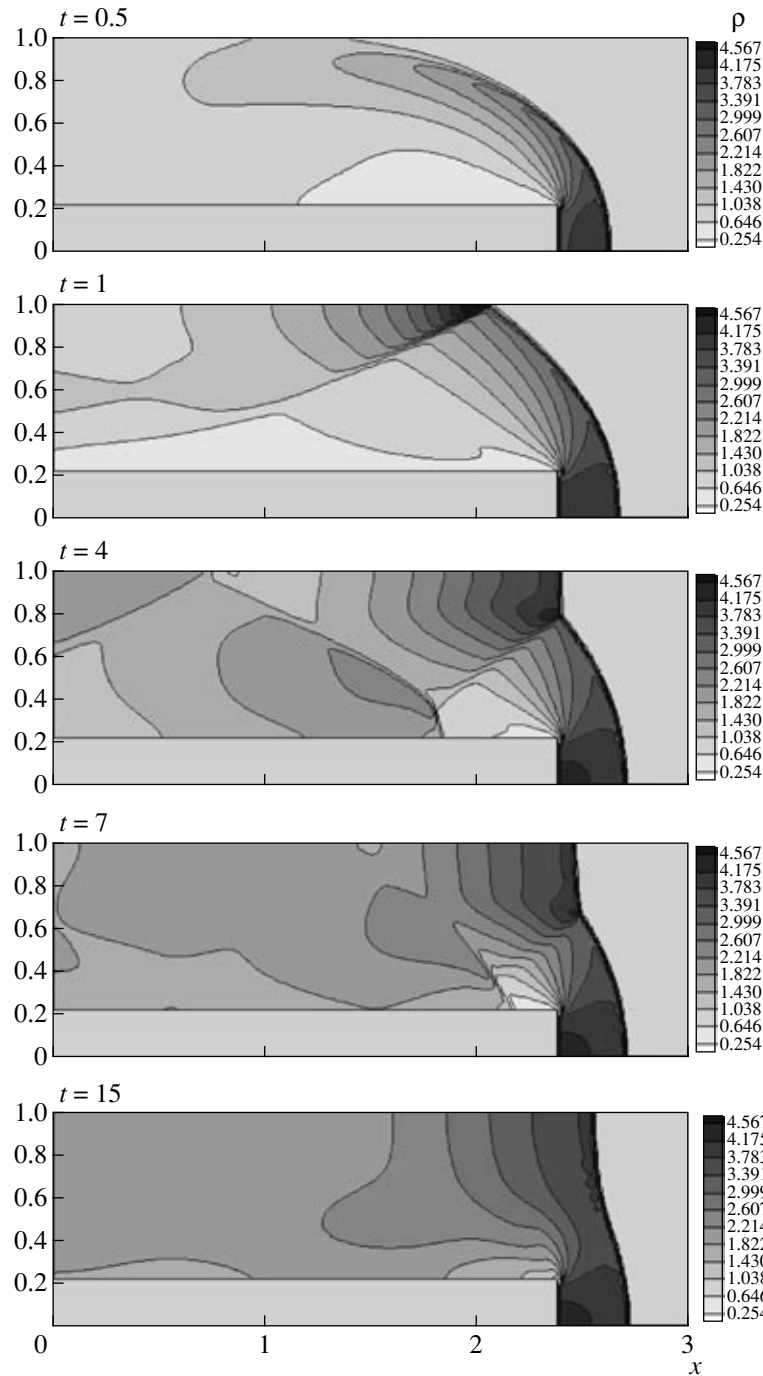


Fig. 2.

In the computation of subsonic flows, the problem arises of setting and numerical implementation of boundary conditions on the free boundaries of the computational domain. Such nonreflecting boundary conditions must not degrade the flow field inside the computational domain and must provide the absorption or transmission of disturbances originating inside the computational domain and arriving at the boundary. As a rule, these boundary conditions are based on Riemann inversions for the corresponding Euler equations and are known as characteristic boundary conditions [10, 11]. They are used in computations of both viscous and inviscid flows. Numerous versions of such conditions and their numerical implementations have been proposed. Nevertheless, their application faces serious difficulties associated with their numerous versions in differential and finite-difference form and with the insufficient mathematical substantiation of these conditions for viscous gas flows.

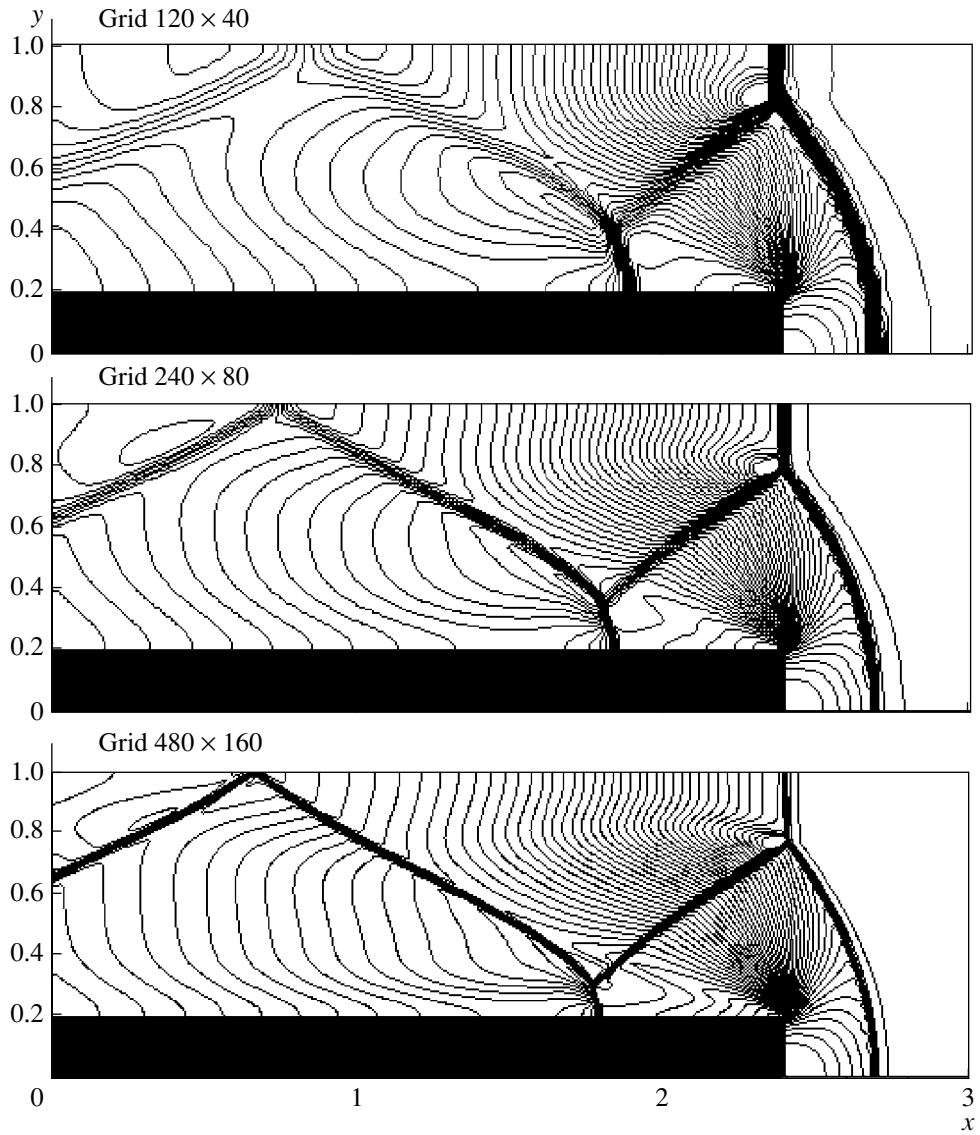


Fig. 3.

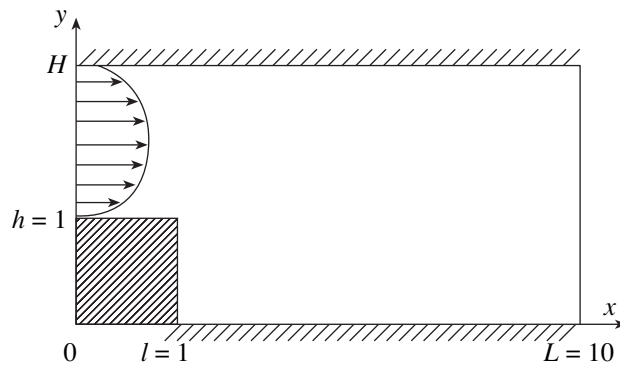


Fig. 4.

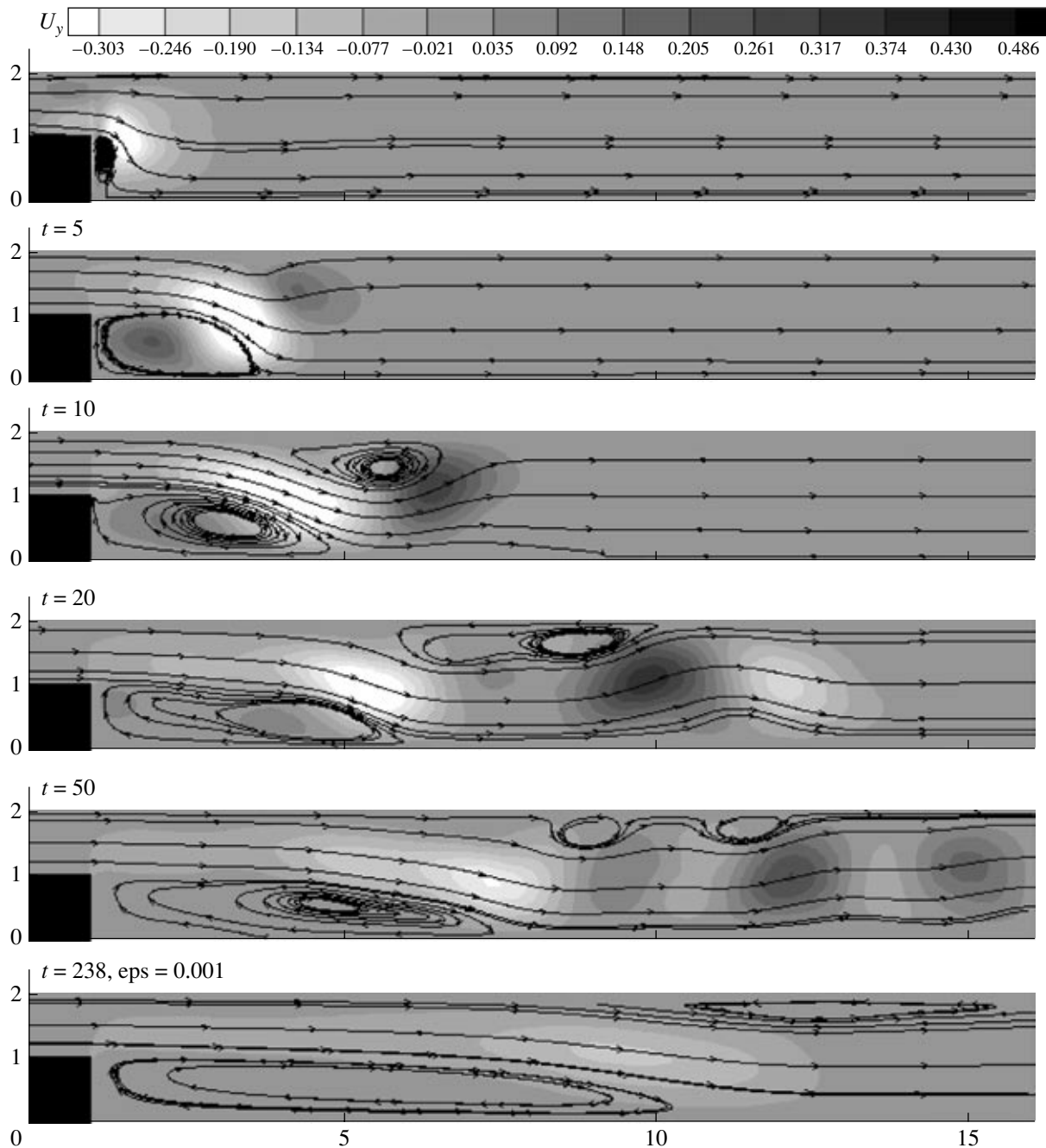


Fig. 5.

Within the framework of the QGD algorithm for setting conditions on free subsonic boundaries, simple and natural boundary conditions can be applied that are similar to those used for viscous incompressible flows. The setting of such conditions is described for the problem of a flow in a channel with a sudden enlargement (see Fig. 4).

Assume that the flow at the inlet of the channel is governed by Poiseuille's equation:

$$u_x(y) = -\frac{\text{Re} \partial p}{2 \partial x} (H-y)(h-y), \quad p = \left(1 - \frac{x}{L}\right) p_1 + \frac{x}{L} p_2.$$

The condition that $u_\infty = 1$ at the inlet is used to calculate the pressure gradient at the inlet of the channel.

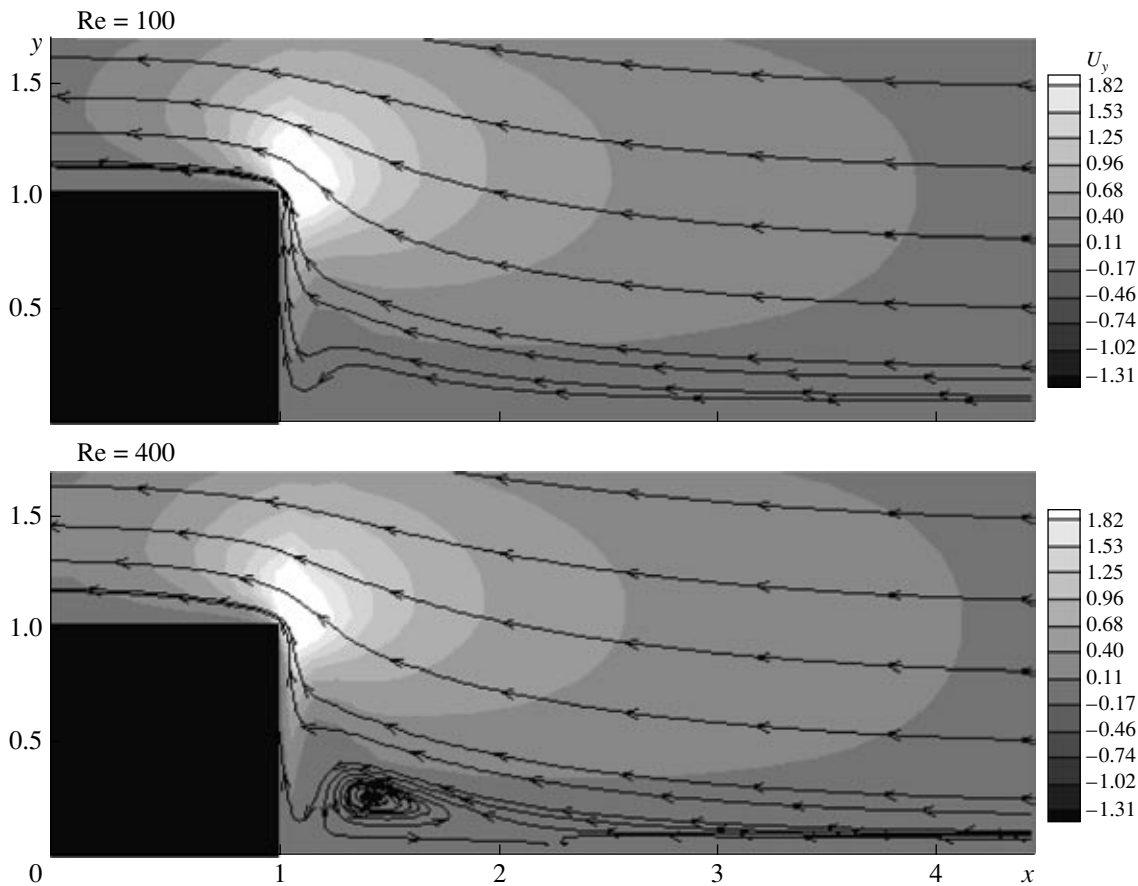


Fig. 6.

To be specific, we set $H/h = 2$. Then,

$$u_x(y) = -6(2 - y)(1 - y), \quad \frac{\partial p}{\partial x} = -\frac{12}{\text{Re}}. \tag{4.1}$$

The inlet boundary conditions (4.1) are supplemented with conditions for the density ($\rho = 1$) and for the vertical velocity ($u_y = 0$).

At the outlet boundary, the mild boundary conditions are specified for the density and velocity components and the pressure is held fixed:

$$\frac{\partial \rho}{\partial x} = 0, \quad \frac{\partial u_x}{\partial x} = 0, \quad \frac{\partial u_y}{\partial x} = 0, \quad p = \frac{1}{\gamma M^2}.$$

On the rigid walls of the channel, we set the no-slip and impermeability conditions and the adiabatic conditions for the temperature (1.19).

The algorithm described was used to compute viscous compressible gas (air) flows (with the parameters $\gamma = 1.4$, $\text{Pr} = 0.373$, $\text{Sc} = 0.746$, and $\omega = 0.74$) in channels with a sudden expansion or contraction at the Reynolds numbers 100, 200, 300, and 400 at M ranging from 0.01 to 0.5. We used uniform spatial grids with the mesh sizes $h_x = h_y = 0.1$ and 0.05. The time steps Δt in dimensionless units were chosen in the range from 10^{-3} to 10^{-4} .

For the flows under consideration, the gradients of density are proportional to M , which allows us to estimate the accuracy of the resulting solution by comparing it with the computations performed in the approximation of a viscous incompressible fluid [12, 13].

In the problem of flow behind a backward-facing step, it was found that the length of the separation region agrees with the results obtained in computations and experiments for a viscous incompressible fluid [12] and the accuracy of the numerical results based on the QGD model virtually does not depend on α in

the range $0.5 < \alpha < 2$. When α lies outside this range, the time step has to be reduced and the number of steps required for achieving a steady state increases. In the analyzed range of the Mach number, the length of the separation region virtually does not depend on the Mach number. A reduction in the Mach number increases the number of steps and the time required for achieving a steady state. Figure 5 displays the process of flow relaxation for $Re = 300$ ($\alpha = 0.5$, $M = 0.1$, a 160×120 grid), namely, the distribution of u_y (shown by shades of gray) and streamlines. It can be seen that disturbances freely cross the outlet boundary of the region.

The flow computations for the channel with a sudden contraction were compared with the results obtained in [13] within the framework of the incompressible Navier–Stokes equations written in terms of stream function and vorticity variables. Figure 6 shows the distribution of u_y and streamlines for the following two versions of a steady flow: $Re = 100$ and 400 ($M = 0.1$, $\alpha = 0.5$, a 50×20 grid). In the first case, no separation flow is formed in front of the step or over it. At $Re = 400$, a vortex is formed in front of the step. The formation of a separation region with increasing Reynolds number and its size agree well with the results of [13].

To conclude, we note that, in our view, the simplicity of implementation and the good accuracy of the numerical algorithms constructed for computing supersonic and subsonic unsteady gas flows are ensured by the special regularizers used in the QGD equations.

ACKNOWLEDGMENTS

The authors are grateful to A.G. Sveshnikov for his interest in and encouragement of this study.

REFERENCES

1. T. G. Elizarova and B. N. Chetverushkin, “Kinetic Models as Applied to the Computation of Gasdynamic Flows,” in *Mathematical Modeling: Processes in Nonlinear Media* (Nauka, Moscow, 1986), pp. 261–278 [in Russian].
2. Yu. V. Sheretov, *Mathematical Modeling of Fluid Flows Based on Quasi-Hydrodynamic and Quasi-Gasdynamic Equations* (Tversk. Gos. Univ., Tver, 2000) [in Russian].
3. Yu. V. Sheretov, “Some Properties of Quasi-Gasdynamic Equations,” in *Applications of Functional Analysis to Approximation Theory* (Tversk. Gos. Univ., Tver, 2000), pp. 134–149 [in Russian].
4. T. G. Elizarova and Yu. V. Sheretov, “Theoretical and Numerical Analysis of Quasi-Gasdynamic and Quasi-Hydrodynamic Equations,” *Zh. Vychisl. Mat. Mat. Fiz.* **41**, 239–255 (2001) [*Comput. Math. Math. Phys.* **41**, 219–234 (2001)].
5. B. N. Chetverushkin, *Kinetically Consistent Schemes in Gas Dynamics* (Mosk. Gos. Univ., Moscow, 1999) [in Russian].
6. Yu. V. Sheretov, “Finite Difference Approximations of Quasi-Gasdynamic Equations for Axisymmetric Flows,” in *Applications of Functional Analysis to Approximation Theory* (Tversk. Gos. Univ., Tver, 2001), pp. 191–207 [in Russian].
7. T. G. Elizarova and M. E. Sokolova, “Numerical Algorithm for Supersonic Flow Computation Based on Quasi-Gasdynamic Equations,” *Vestn. Mosk. Gos. Univ., Ser. 3: Fiz. Astron.*, No. 1, 10–15 (2004).
8. P. Woodward and P. J. Collela, “The Numerical Simulation of Two-Dimensional Fluid Flow with Strong Shock,” *J. Comput. Phys.*, No. 5, 115–173 (1984).
9. I. A. Graur, “Method of Quasi-Gasdynamic Splitting for Solving the Euler Equations,” *Zh. Vychisl. Mat. Mat. Fiz.* **41**, 1583–1596 (2001) [*Comput. Math. Math. Phys.* **41**, 1506–1518 (2001)].
10. R. D. Richtmyer and K. W. Morton, *Difference Methods for Initial-Value Problems* (Wiley, New York, 1967; Mir, Moscow, 1980).
11. M. A. Il’gamov and A. N. Gil’manov, *Nonreflecting Conditions on the Boundary of the Computational Domain* (Fizmatlit, Moscow, 2003) [in Russian].
12. B. F. Armaly, F. Durst, J. C. F. Pereira, and B. Schonung, “Experimental and Theoretical Investigation of Backward-Facing Step Flow,” *J. Fluid Mech.*, No. 127, 473–496 (1983).
13. R. V. Mei and A. Plotkin, “Navier–Stokes Solutions for Some Laminar Incompressible Flows with Separation Inforward Stepgeometries,” AIAA Paper, No. 8, 110 (1986).